Dilepton gauge bosons: Present status and future prospects

Paul H. Frampton and Daniel Ng
Institute of Field Physics, Department of Physics and Astronomy, University of North Carolina, Chapel Hill, North Carolina 27599-3255
(Received 26 December 1991)

Dilepton gauge bosons which appear in a class of unified models are studied both from the point of view of existing data and of future experiments. Present data allow masses only above 120 GeV. Future experiments in e^+e^- scattering can improve this bound to 600 GeV (CERN e^+e^- collider LEP II with $\sqrt{s}=200$ GeV) and to 1500 GeV (Next Linear Collider e^+e^- with $\sqrt{s}=500$ GeV). The process $e^-e^-\to\mu^-\mu^-$ could provide an excellent signature for the existence of dilepton gauge bosons in an e^-e^- collider, even for $\sqrt{s}=100$ GeV.

PACS number(s): 14.80.Er, 12.15.Cc, 12.15.Ji, 13.10.+q

I. INTRODUCTION

The standard model (SM) of strong and electroweak interactions is extremely successful. The biggest question confronting particle physics at present is, where will we find evidence for physics distinctively beyond the SM? Popular theoretical directions beyond the SM include (in no particular order) supersymmetry, technicolor, and grand unification. So far, no persuasive experimental support for any of these ideas has been forthcoming. In the foreseeable future, we shall explore thoroughly the energy region up to and beyond $E=1$ TeV, and it is therefore important to explore theoretically the widest variety of possible (and plausible) scenarios.

One class of particle which appears in a wide class of theories is the dilepton gauge boson. For example, in SU(15) grand unification [1], there appear dilepton gauge particles [2] in doublets of weak SU(2): $(X^{--}X^{-})$ and antiparticles $(X^{++}X^{+})$ which are part of a gauged leptonic $SU(3)_l$ under which $(\nu_e e^- e^+)_L$ and the corresponding leptons of the second and third families transform as a triplet. These states more generally appear in any framework where the leptonic electroweak $SU(2)\times U(1)$ is part of an $SU(3)_l$ and where B (baryon number) and L (lepton number) are conserved. The mass M_X, generated by the Higgs mechanism, depends on the breaking scale called M_A in Ref. [1] and which may be as low as the weak scale. Thus M_X can be ~ 100 GeV and hence pertinent to lepton accelerator experiments. Since they are gauge particles, their coupling to leptons is prescribed to be g_{3l} of $SU(3)_l$ and this means their contributions to weak processes are comparable in order of magnitude, up to a power of M_Z/M_X, to that of $Z, W^{\pm}$ mediated-weak processes.

Our aim in this paper is twofold. In Sec. II we place lower-mass bounds on M_X from existing data on weak processes. Second, in Sec. III there are predictions for e^+e^- and e^-e^- colliders at higher energy. Finally, in Sec. IV we make some concluding remarks.

II. LOWER LIMITS ON DILEPTON MASS FROM EXISTING DATA

Assuming that the dilepton (X) is gauge coupled to leptons as dictated by the gauge group SU(15) or $SU(3)_l$ discussed in the Introduction, we may study existing experimental data to place lower limits on the allowed dilepton mass. Since such a dilepton would contribute to weak interactions with a coupling strength of comparable order of magnitude to that for $W^{\pm}$ and Z, we expect such a lower bound to be at least the mass of W and Z. This expectation will be borne out by our analysis.

In this section we study the constraints from the following experiments: (A) muon decay, (B) low-energy weak neutral current, and (C) Bhabha e^+e^- scattering.

Let us first write the dilepton interaction, which is explicitly given by the interaction Lagrangian

$$\begin{aligned} L_X=&\frac{g_{3l}}{\sqrt{2}}X_\mu^{++}e^T C\gamma^\mu\left[\frac{1-\gamma_5}{2}\right]e \\ &+\frac{g_{3l}}{\sqrt{2}}X_\mu^{--}\bar{e}\gamma^\mu\left[\frac{1-\gamma_5}{2}\right]C\bar{e}^T \\ &+\frac{g_{3l}}{\sqrt{2}}X_\mu^{+}e^T C\gamma^\mu\left[\frac{1-\gamma_5}{2}\right]\nu_e \\ &+\frac{g_{3l}}{\sqrt{2}}X_\mu^{-}\bar{\nu}_e\gamma^\mu\left[\frac{1-\gamma_5}{2}\right]C\bar{e}^T, \end{aligned} \tag{2.1}$$

where X^{--}, X^{-} and their antiparticles X^{++}, X^{+} are the massive dileptons which arise when $SU(3)_l$ is spontaneously broken at the scale $\mu=M_A$. The coupling g_{3l} is given approximately by $g_{3l}=1.19e$, where e is the magnitude of the electronic charge.

In the first two (doubly charged) currents in Eq. (2.1), the vector couplings vanish by Fermi statistics, and so we are left with the simplification

$$L_X=-\frac{g_{3l}}{\sqrt{2}}X_\mu^{++}e^T C\gamma^\mu\gamma_5 e-\frac{g_{3l}}{\sqrt{2}}X_\mu^{--}\bar{e}\gamma^\mu\gamma_5 C\bar{e}^T$$
$$+\frac{g_{3l}}{\sqrt{2}}X_\mu^{+}e^T C\gamma^\mu\left[\frac{1-\gamma_5}{2}\right]\nu_e$$
$$+\frac{g_{3l}}{\sqrt{2}}X_\mu^{-}\bar{\nu}_e\gamma^\mu\left[\frac{1-\gamma_5}{2}\right]C\bar{e}^T . \quad (2.2)$$

With this interaction we can now analyze the experimental constraints on M_X from the various experiments mentioned above.

A. Muon decay

The branching ratio for $\mu^-\to e^-\nu_e\bar{\nu}_\mu$ relative to the standard decay mode $\mu^-\to e^-\bar{\nu}_e\nu_\mu$ has been measured, from the crossed process $\bar{\nu}_\mu e^-\to\bar{\nu}_e\mu^-$ [3], to be less than 5%. This corresponds to the limit

$$\frac{M_X}{g_{3l}}>260\ \text{GeV} , \quad (2.3)$$

which translates into $M_X>90$ GeV if $g_{3l}=1.19e$ is used.

B. Neutral-current experiments

The singly charged dilepton will contribute to $\nu_e e^-$ and $\bar{\nu}_e e^-$ scattering experiments. The effective Lagrangian for these low-energy processes is given by

$$L_{\rm NC}=-\frac{G_F}{\sqrt{2}}\nu_e\gamma_\mu(1-\gamma_5)\nu_e\bar{e}\gamma^\mu$$
$$\times[a_L(1-\gamma_5)+a_R(1+\gamma_5)]e , \quad (2.4)$$

with

$$a_L=(-\tfrac{1}{2}+\sin^2\theta_W)+1 , \quad (2.5)$$

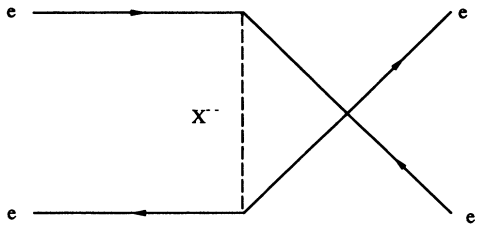

FIG. 1. Feynman diagram of the doubly charged dilepton X^{--} contribution to the process $e^+e^-\to e^+e^-$.

$$a_R=\sin^2\theta_W-\frac{g_{3l}^2M_W^2}{M_X^2g^2} , \quad (2.6)$$

where G_F is the Fermi constant and g is the $SU(2)_L$ coupling. Experimental results [4] on $\nu_e e^-$ and $\bar{\nu}_e e^-$ scattering give rise to the values

$$a_R^2=0.0084\pm0.031 , \quad (2.7)$$

which correspond to

$$\frac{M_X}{g_{3l}}>600\ \text{GeV} , \quad (2.8)$$

at a two-standard-deviation level. This would translate into $M_X>230$ GeV. However, this constraint may not be as trustworthy as the others we derive because the numbers of events obtained are very low and hence the reliability of the error in Eq. (2.7) is somewhat unclear.

C. Bhabha scattering

In e^+e^- scattering a doubly charged dilepton contributes by u-channel exchange, which adds to the s- and t-channel exchanges of γ and Z (see Fig. 1). The contribution to the amplitude is given by

$$A_X=-\left[\frac{g_{3l}}{\sqrt{2}}\right]^2\frac{1}{u-M_X^2}\bar{u}(p_3)\gamma_\mu\gamma_5 C\bar{v}^T(p_2)v^T(p_4)C\gamma^\mu\gamma_5 u(p_1) , \quad (2.9)$$

where the sign arises from the order of the fermion fields relative to the standard s-channel exchange of γ and Z. With Fierz reordering, Eq. (2.9) can be rewritten as

$$A_X=-\left[\frac{g_{3l}}{\sqrt{2}}\right]^2\frac{1}{u-M_X^2}\left[\bar{u}(p_3)\gamma_\mu\frac{1+\gamma_5}{2}v(p_4)\bar{v}(p_2)\gamma^\mu\frac{1-\gamma_5}{2}u(p_1)+\bar{u}(p_3)\gamma_\mu\frac{1-\gamma_5}{2}v(p_4)\bar{v}(p_2)\gamma^\mu\frac{1+\gamma_5}{2}u(p_1)\right.$$
$$-\bar{v}(p_2)\gamma_\mu\frac{1+\gamma_5}{2}v(p_4)\bar{u}(p_3)\gamma^\mu\frac{1-\gamma_5}{2}u(p_1)$$
$$\left.-\bar{v}(p_2)\gamma_\mu\frac{1-\gamma_5}{2}v(p_4)\bar{u}(p_3)\gamma^\mu\frac{1+\gamma_5}{2}u(p_1)\right] , \quad (2.10)$$

where $u=-(s/2)(1+\cos\theta)$, with $\sqrt{s}$ and θ are the total energy and scattering angle in the center-of-mass frame, respectively.

For $M_X\gg\sqrt{s}$, Eq. (2.10) is identical to a four-fermion interaction with $\eta_{LL}=\eta_{RR}=0$ and $\eta_{LR}=\eta_{RL}=1$ using the definitions of Ref. [5]. From the experimental results [6] of the DESY e^+e^- collider PETRA at $\sqrt{s}=35$ GeV and an integrated luminosity of 87 pb^{-1}, we obtain

$$\sqrt{2}\frac{M_X}{g_{3l}}=\frac{\Lambda_{LR}}{\sqrt{4\pi}}>\frac{1.7\ \text{TeV}}{\sqrt{4\pi}}\ , \tag{2.11}$$

which implies

$$\frac{M_X}{g_{3l}}>340\ \text{GeV}\ , \tag{2.12}$$

at 95% confidence level. In Eq. (2.11), Λ_{LR} is the composite scale at which the four-fermion interaction is induced.

A similar study of the lower bound on the compositeness scale was carried out at KEK TRISTAN [7], but despite the higher center-of-mass energy, those data may not allow a better bound than Eq. (2.12) because the integrated luminosity is lower than that of PETRA. The data from the CERN e^+e^- collider LEP with an even higher center-of-mass energy do not allow a stronger bound because the results are so dominated by the s-channel Z pole.

From Eq. (2.12) the lower bound on the dilepton mass is 120 GeV. This is our most solid limit. Note that it still allows a branching fraction of 2% for the "wrong" muon decay $\mu^-\to e^-\nu_e\bar{\nu}_\mu$.

III. FUTURE EXPERIMENTS ON BHABHA AND MOELLER SCATTERING

First, we consider Bhabha scattering $e^+e^-\to e^+e^-$. Combining Eq. (2.9) with the s- and t-channel exchange of γ and Z, the total transition amplitude may be written

$$\begin{aligned}A(e^+e^-\to e^+e^-)&=\frac{e^2}{s}G_{BA}(s)\bar{u}(p_3)\gamma_\mu P_B v(p_4)\bar{v}(p_2)\gamma^\mu P_A u(p_1)\\&\quad-\frac{e^2}{s}G_{BA}(t)\bar{v}(p_2)\gamma_\mu P_B v(p_4)\bar{u}(p_3)\gamma^\mu P_A u(p_1)\ ,\end{aligned} \tag{3.1}$$

for $A,B=L,R$ and where

$$G_{BA}(w)=\frac{s}{w}+\frac{g_B g_A}{e^2}\frac{s}{w-M_Z^2}+(\delta_{BA}-1)\left[\frac{g_{3l}}{\sqrt{2}e}\right]^2\frac{s}{u-M_X^2}\ , \tag{3.2}$$

where $P_L=(1-\gamma_5)/2$, $P_R=(1+\gamma_5)/2$, $g_L=-e\cot 2\theta_W$, $g_R=e\tan\theta_W(\sin^2\theta_W=0.23)$, $s=(p_1+p_2)^2$, $t=(p_1-p_3)^2$, and $u=(p_1-p_4)^2$.

The differential cross section is given by

$$\frac{d\sigma(e^+e^-\to e^+e^-)}{d\cos\theta}=\frac{\pi\alpha^2}{2s}\left[[|G_{LR}(t)|^2+|G_{RL}(t)|^2]+\left[\frac{t}{s}\right]^2[|G_{LR}(s)|^2+|G_{RL}(s)|^2]+\left[\frac{u}{s}\right]^2[|G_{LL}(s)+G_{LL}(t)|^2+|G_{RR}(s)+G_{RR}(t)|^2]\right]\ , \tag{3.3}$$

where θ is the scattering angle between the initial and final electron in the center-of-mass frame. In Fig. 2 we plot $d\sigma(e^+e^-\to e^+e^-)/d\cos\theta|_{\text{SM}}$, which is given by Eqs. (3.1)–(3.3) with $g_{3l}=0$ or equivalently $M_X=\infty$, versus $\cos\theta$ for LEP II ($\sqrt{s}=200$ GeV) and NLC (Next Linear Collider with $\sqrt{s}=500$ GeV).

To find a departure from the standard model, we plot the ratio ρ^{+-} of Eq. (3.3) to the corresponding differential cross section of the SM,

$$\rho^{+-}=\frac{d\sigma(e^+e^-\to e^+e^-)/d\cos\theta}{d\sigma(e^+e^-\to e^+e^-)/d\cos\theta|_{\text{SM}}}\ , \tag{3.4}$$

as a function of $\cos\theta$. In Figs. 3(a) and 3(b), ρ^{+-} of Eq. (3.4) is plotted versus $\cos\theta$ for LEP II and the NLC, respectively, with selected choices of M_X. In relation to Fig. 3, let us assume that the integrated luminosities for LEP II and the NLC are 1 and 10 fb^{-1}/yr, respectively. The uncertainities for both experiments are approximately given by $1\sqrt{N}\approx 5\%$ if we take the bin size $\delta\cos\theta=0.1$ (here N is the number of events/yr). If we require ρ^{+-} to be at least 10% different from unity for a detectable signal, we find that LEP II and the NLC can probe for dileptons with masses up to 600 and 1500 GeV, respectively, assuming gauge couplings to e^-e^- of the strength discussed in the Introduction.

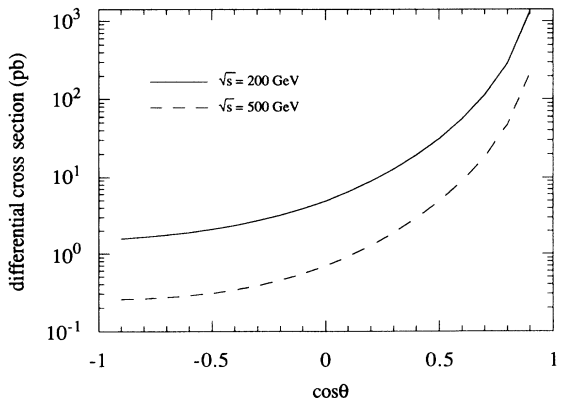

FIG. 2. Differential cross section for $e^+e^-\to e^+e^-$ in the standard model as a function of $\cos\theta$ at the center-of-mass energies $\sqrt{s}=200$ and 500 GeV.

Finally, we turn to the very interesting case of Moeller scattering $e^-e^-\to e^-e^-$. The amplitude for Moeller scattering is simply related by crossing symmetry to that of Bhabha scattering. The transition amplitude for Moeller scattering is thus given by

$$A(e^-e^-\to e^-e^-) = \frac{e^2}{s}H_{BA}(t)\bar{u}(p_4)\gamma_\mu P_B u(p_2)\bar{u}(p_3)\gamma^\mu P_A u(p_1) - \frac{e^2}{s}H_{BA}(u)\bar{u}(p_3)\gamma_\mu P_B u(p_2)\bar{u}(p_4)\gamma^\mu P_A u(p_1)\ , \tag{3.5}$$

with

$$H_{BA}(w)=\frac{s}{2}+\frac{g_B g_A}{e^2}\frac{s}{w-M_Z^2} + (\delta_{BA}-1)\left[\frac{g_{3l}}{\sqrt{2}e}\right]^2\frac{s}{s-M_X^2+iM_X\Gamma_X}\ . \tag{3.6}$$

The differential cross section $e^-e^-\to e^-e^-$ is then given by

$$\frac{d\sigma(e^-e^-\to e^-e^-)}{d\cos\theta}=\frac{\pi\alpha^2}{4s}\left[[|H_{LL}(t)+H_{LL}(u)|^2+|H_{RR}(t)+H_{RR}(u)|^2] + \left[\frac{u}{s}\right]^2[|H_{LR}(t)|^2+|H_{RL}(t)|^2]+\left[\frac{t}{s}\right]^2[|H_{LR}(u)|^2+|H_{RL}(u)|^2]\right]\ . \tag{3.7}$$

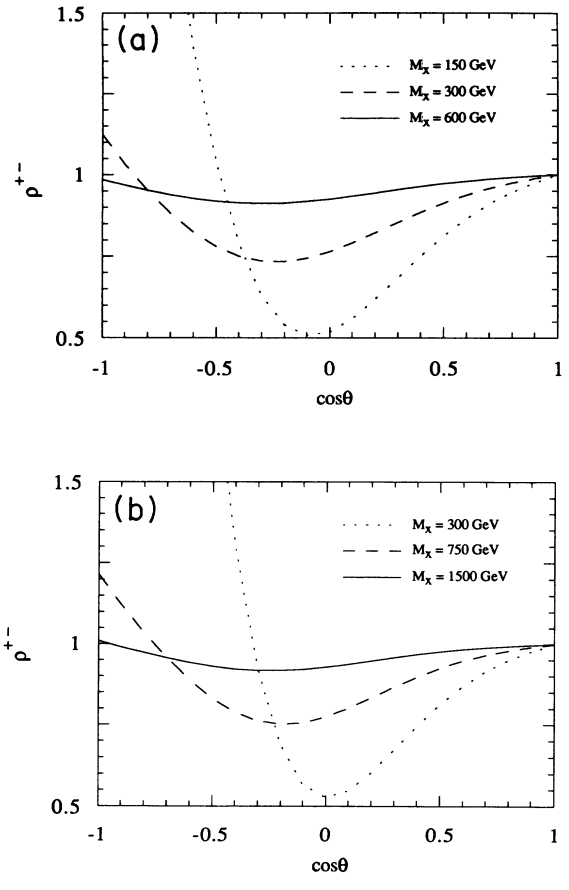

FIG. 3. Ratio ρ^{+-} of the differential cross section for $e^+e^-\to e^+e^-$ in the presence of X^{--} to that of the standard model as a function of $\cos\theta$ for (a) $\sqrt{s}=200$ GeV and $M_X=150$, 300, and 600 GeV; (b) $\sqrt{s}=500$ GeV and $M_X=300$, 800, and 1500 GeV.

The standard-model prediction at $\sqrt{s}=500$ GeV is plotted versus $\cos\theta$ in Fig. 4. The $\cos\theta$ distribution relative to that of the SM, ρ^{--}, is displayed in Fig. 5 for various values of M_X at $\sqrt{s}=500$ GeV. In connection with this graph, note that an integrated luminosity of 10 fb^{-1} would yield approximately 10^4 events per $\delta\cos\theta=0.1$. This implies an uncertainty $\sim 1\%$, and so the 2% variance from the standard model at $M_X=800$ GeV is detectable in a 500 GeV NLC e^-e^- machine.

As the doubly charged dilepton X^{--} contributes to the process $e^-e^-\to e^-e^-$ by s-channel exchange, the resonance at $\sqrt{s}=M_X$ shows up dramatically. The width of X^{--} is calculated to be 3 times $(g_{3l}^2/48\pi)M_X$, where the factor 3 counts families. Taking $M_X=500$ GeV, for example, the total cross section of this process with $|\cos\theta|<0.8$ is plotted in Fig. 6.

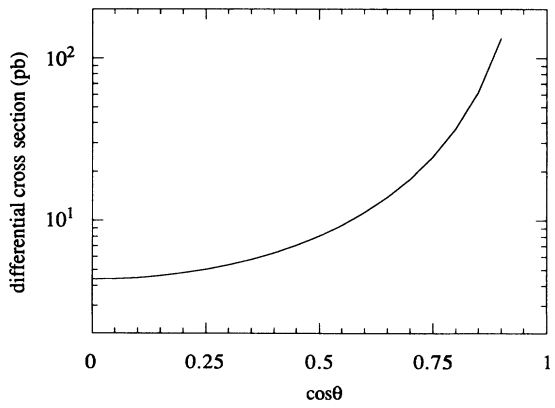

FIG. 4. Differential cross section for the process $e^-e^-\to e^-e^-$ in the standard model as a function of $\cos\theta$ at $\sqrt{s}=500$ GeV.

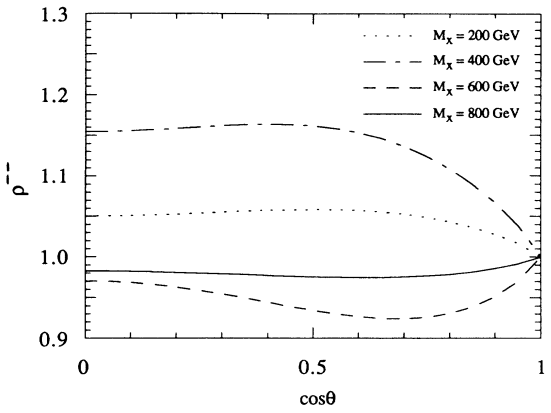

FIG. 5. Ratio ρ^{--} of the differential cross section for $e^-e^- \to e^-e^-$ in the presence of X^{--} to that of the standard model as a function of $\cos\theta$ for $M_X = 200$, 400, 600, and 800 GeV.

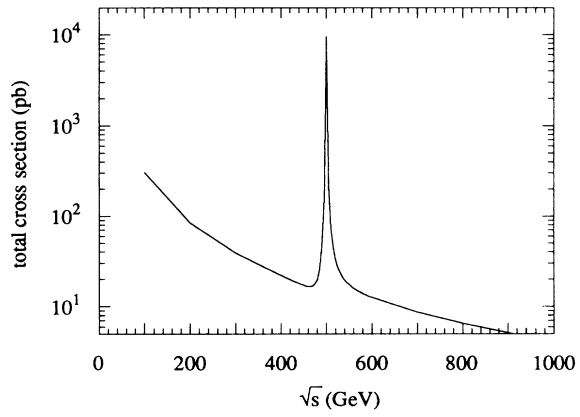

FIG. 6. Total cross section for $e^-e^- \to e^-e^-$ in the presence of X^{--} as a function of $\sqrt{s}$, where $|\cos\theta| < 0.8$ is used and $M_X = 500$ GeV is assumed.

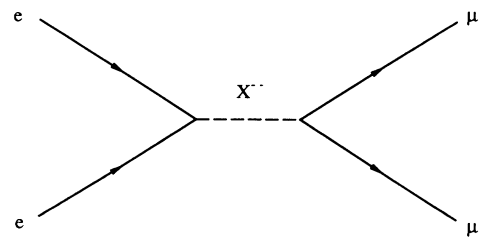

FIG. 7. Feynman diagram for the process $e^-e^- \to \mu^-\mu^-$ induced by X^{--}.

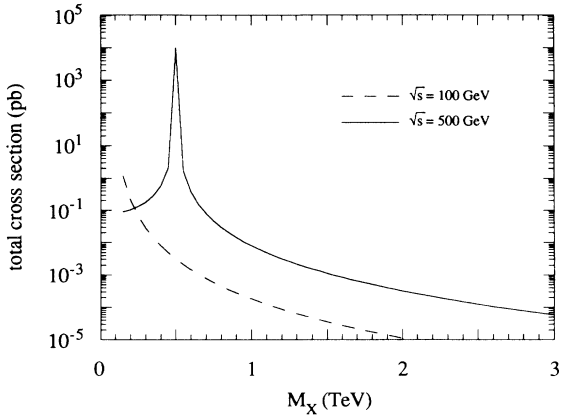

FIG. 8. Total cross section for $e^-e^- \to \mu^-\mu^-$ induced by X^{--} as a function of M_X for $\sqrt{s} = 100$ and 500 GeV, where $|\cos\theta| < 0.8$ is used.

Of special interest is the capability of an e^-e^- machine to seek an exotic process $e^-e^- \to \mu^-\mu^-$ corresponding to the Feyman diagram shown in Fig. 7. In Fig. 8 a plot is shown of the total cross section of this process with $|\cos\theta| < 0.8$ vs M_X for $\sqrt{s} = 500$ GeV (solid curve) and for $\sqrt{s} = 100$ GeV (dashed curve). In a NLC (e^-e^- with $\sqrt{s} = 500$ GeV) with an integrated luminosity 10 fb^{-1}, there will be five events for $M_X = 1.8$ TeV. The dashed curve in Fig. 8 is suggestive of the Stanford Linear Collider (SLC) in an e^-e^- Moeller mode; we note that e^-e^- in collider mode has not been investigated at center-of-mass energies above 1.112 GeV [8]. For an integrated luminosity 1 fb^{-1}, there would be five events for $M_X = 400$ GeV. Such a signal has zero background from processes predicted by the standard model in which electron and muon lepton numbers are separately conserved.

IV. SUMMARY

From a class of theoretical models, there is the prediction of difermions on the order of the 10^2-GeV range; these may be diquarks, leptoquarks, or dileptons. In this paper we have focused on dileptons as of particular experimental interest.

From existing data we have placed a firm lower bound of 120 GeV on gauge-coupled dileptons. This is still consistent with muon decay $\mu^- \to e^-\nu_e\bar{\nu}_\mu$ occurring at the 1% or 2% level.

In future e^+e^- colliders we find that LEP II ($\sqrt{s} = 200$ GeV) and the NLC ($\sqrt{s} = 500$ GeV) can detect dileptons with masses up to 600 and 1500 GeV, respectively. Electron-electron collisions at the center-of-mass energies $\sqrt{s} = 100$ GeV (500 GeV) could be sensitive to M_X in the unexplored mass region up to 400 GeV (1800 GeV) by the characteristic $e^-e^- \to \mu^-\mu^-$ signature.

ACKNOWLEDGMENTS

This work was supported in part by U.S. Department of Energy Grant No. DE-FG05-85ER-40219.

[1] P. H. Frampton and B.-H. Lee, Phys. Rev. Lett. **64**, 619 (1990).
[2] P. H. Frampton, Mod. Phys. Lett. A **7**, 559 (1992).
[3] CHARM Collaboration, F. Bergsma *et al.*, Phys. Lett. **122B**, 465 (1983).
[4] G. L. Fogli, Europhys. Lett. **4**, 527 (1987).
[5] E. J. Eichten *et al.*, Phys. Rev. Lett. **50**, 811 (1985).
[6] CELLO Collaboration, H. J. Behrend *et al.*, Z. Phys. C **51**, 149 (1991).
[7] T. Nozaki, in Proceedings of the 29th Rencontre de Moriond, 1989 (unpublished); A. Maki, KEK Report No. 91-100, 1991 (unpublished).
[8] W. C. Barber *et al.*, Phys. Rev. D **3**, 2796 (1971).